Hindawi
Journal of Food Biochemistry
Volume 2023, Article ID 5273349, 16 pages
https://doi.org/10.1155/2023/5273349

*Research Article*

# Flavonoids from *Lophatherum gracile* Brongn. Ameliorate Liver Damages in High-Fat Diet and Streptozotocin-Induced Diabetic Mice by Regulating PI3K/AKT and NF-Kappa B Pathways

**Jian-Hua Zheng**,[1] **Song-Xia Lin**,[2] **Xiao-Yi Li**,[2] **Chun-Yan Shen**,[2] **Shao-Wei Zheng**,[3] **and Wen-Bin Chen**[1]

[1]*Department of Traditional Chinese Medicine, Huizhou First Hospital, Guangdong Medical University, Huizhou 516003, China*
[2]*School of Traditional Chinese Medicine, Southern Medical University, Guangzhou 510515, China*
[3]*Department of Orthopaedic, Huizhou First Hospital, Guangdong Medical University, Huizhou 516003, China*

Correspondence should be addressed to Chun-Yan Shen; shenchunyan@smu.edu.cn, Shao-Wei Zheng; zswljq@126.com, and Wen-Bin Chen; hzzy_cwb@163.com

Received 21 April 2023; Revised 25 August 2023; Accepted 23 September 2023; Published 6 October 2023

Academic Editor: Walid Elfalleh



Inflammation and metabolic disorders are crucial factors that induce type 2 diabetes mellitus (T2DM). *Lophatherum gracile* Brongn. (*L. gracile*) has been popularly consumed as folk medicine and dietary supplement for the treatment of fever and inflammatory-associated diseases. Flavonoids are the major constituents of *L. gracile* with various pharmacological effects. However, the protective effects of flavonoids from leaves of *L. gracile* against T2DM, as well as the potential mechanisms, were not yet elucidated. In the present study, the total flavonoid content of *L. gracile* (LGBF) with higher flavonoid content and pancreas lipase inhibitory activity was extracted and screened from the leaves of *L. gracile*. Twelve flavonoid compounds were identified in LGBF by liquid LC-MS analysis. Network pharmacology identified seven potential flavonoid compounds and 10 core targets associated with T2DM. GO and KEGG pathway enrichment analysis indicated that PI3K/AKT and inflammation-related pathways might occupy core status. Molecular docking results showed that the active constituents of LGBF had a good binding activity with key targets. Furthermore, high-fat diet (HFD) and streptozotocin (STZ)-induced diabetic mice were developed and treated with LGBF for experimental validation. The data showed that LGBF intervention potently improved the lipid profiles and insulin sensitivity of HFD and STZ-induced mice. Hepatic inflammation and lipid accumulation were also partially reversed by LGBF intervention. Further assays confirmed that LGBF administration significantly increased PI3K and AKT phosphorylation, while reducing IL-1$\beta$ expression and NF-$\kappa$B P65 phosphorylation in the liver of mice. In conclusion, LGBF administration could relieve liver damage in diabetic mice via regulating PI3K/AKT and NF-$\kappa$B pathways.

## 1. Introduction

Type 2 diabetes mellitus (T2DM) is a common chronic metabolic disease characterized by hyperglycemia, hyperlipidemia, and insulin resistance (IR) [1, 2]. Accumulating studies have suggested that T2DM is a great risk factor for many human diseases, such as nonalcoholic fatty liver disease and cardiovascular diseases [3]. The prevalence of T2DM has become a global public health burden and attracted much attention. Unfortunately, available therapeutic strategies for the treatment of T2DM and its associated complications exhibit limited efficacy and the side effects are unsatisfactory [4].

It is generally accepted that T2DM is usually accompanied by liver injuries. Excess accumulation of ectopic lipids in the liver of T2DM could activate the inflammatory signaling pathway, thus leading to hepatic inflammation [5]. For example, trilobatin was proven to alleviate the liver damage in high-fat diet (HFD) and streptozotocin (STZ)-induced diabetic mice by reducing the expression of NLRP3

and nuclear factor-kappa B (NF-$\kappa$B) phosphorylation [6]. The phosphatidylinositol-3-kinase (PI3K)/protein kinase B (AKT) pathway also plays a critical role in many tissues during the development of T2DM. In support, Dou et al. showed that camel whey protein significantly prevented liver injuries in T2DM rats by activating the PI3K/AKT pathway [7].

*Lophatherum gracile* Brongn. (*L. gracile*), a perennial herb belonging to the family Gramineae, has been commonly used for treating fever and inflammatory-associated diseases in traditional Chinese medicine [8]. As listed in Chinese Pharmacopoeia, *L. gracile* has various pharmacological effects, including clearing heat fire, promoting diuresis, relieving stranguries, and alleviating heart stress, mouth sores, and restlessness. *L. gracile* has also been popularly consumed as a dietary supplement, which is an important natural additive in the "Wong Lo Kat herbal tea" [9]. The leaves of *L. gracile* contain many constituents, such as polysaccharides, phenolic acids, terpenoids, and especially flavonoids. Numerous studies have demonstrated that flavonoids from *L. gracile* have broad pharmacological activities, such as anti-inflammatory and antioxidant effects [8, 10]. For example, it was found that flavonoids from *L. gracile* showed significant anti-inflammatory potential by inhibiting MAPK and NF-$\kappa$B phosphorylation at the cellular level [10, 11]. However, the protective effects of flavonoids from leaves of *L. gracile* against T2DM, as well as the potential mechanisms, were not yet elucidated.

In the present study, different fractions were isolated and purified from the leaves of *L. gracile* by AB-8 resin column chromatography. The flavonoid content and pancreas lipase inhibitory activity were investigated to screen the fraction with a greater flavonoid content and higher pancreas lipase inhibitory activity, named as LGBF. The major constituents in LGBF were characterized by the LC-MS assay. Then, network pharmacology and molecular docking strategies were employed to predict the potential effective constituents, target genes, and pathways of LGBF against T2DM. Furthermore, HFD and STZ-induced diabetic mice were established and treated with LGBF to investigate and verify the antidiabetic activities and action mechanisms of LGBF. Especially, the protective effects of LGBF against liver damage were determined. The results suggested that LGBF was a promising candidate for the prevention and treatment of liver injuries in T2DM.

## 2. Materials and Methods

*2.1. Materials and Reagents.* The leaves of *L. gracile* were purchased from the Qingping traditional Chinese medicine market (Guangzhou, China) and identified by Professor Chun-Yan Shen (School of Traditional Chinese Medicine, Southern Medical University, Guangzhou, China). Before the study, the leaves of *L. gracile* were dried and ground into an ultrafine powder using a micropulverizer (BFM-6B-III).

Total cholesterol (TC) and triglyceride (TG) were obtained from Nanjing Jiancheng Bioengineering Research Institute (Nanjing, China). Mouse insulin kit was purchased from Jiangsu Jingmei Biotechnology Co. (Jiangsu, China), and interleukin-1$\beta$ (IL-1$\beta$, #12507), p-NF-$\kappa$B-P65 (#3303), p-PI3K (#4228), and p-AKT (#4060) were all acquired from Cell Signaling Technologies (Beverly, MA). ACCU-CHEK Performa was purchased from Roche Diagnostics GmbH (Germany). The rest of the reagents and consumables were of standard laboratory grade and can be obtained commercially.

*2.2. Extraction and Purification.* The leaves of *L. gracile* were dried in an oven (101-3AB, Tianjin Test Instrument Co., Ltd, Tianjin, China) overnight at 45°C. Subsequently, the dried leaves were ground in a BFM-6B-III type micropulverizer (Jinan Billion Powder Engineering Co., Ltd., Shandong, China) and passed through 80 mesh sieves. After 20 min of vibration mill at 4°C and 380 V, the resulting superfine-ground powders were sieved through an 80-mesh screen for later study. 200 mg of ultrafine powder was refluxed with 70% ethanol (1 : 15, v/v) at 100°C for 3 h for 3 times. The yielding 70% ethanol extracts were combined, concentrated under reduced pressure, and dried at 45°C in an oven. Then, the dried 70% ethanol extracts were dissolved in distilled water and further subjected to an AB-8 resin column chromatography, followed by elution with distilled water, 30% ethanol, 50% ethanol, 70% ethanol, and 95% ethanol, respectively. The total flavonoid contents of these eluents were determined according to the method reported by our published research with rutin as a standard [12].

*2.3. Pancreas Lipase Assay.* The pancreas lipase assay was performed according to the previous method with minor modifications [13]. First, 50 mg of pancreatic lipase was dissolved in 50 mL Tris-HCl buffer (0.1 M, pH 7.0, containing 5 mM of calcium chloride) and centrifuged at 4000 rpm (4°C) for 15 min to collect the supernatants. Then, the sample solution (0.25 to 4.0 mg/mL, dissolved in distilled water) was mixed with 50 $\mu$L of the pancreatic lipase solution and incubated at 37°C for 20 min. Afterwards, the pNPB solution (50 $\mu$L, 6 mM, dissolved in Tris-HCl buffer) was added and the incubation was continued at 37°C for 30 min. Finally, the absorbance was measured at 405 nm. Orlistat was used as the positive control. The pancreatic lipase inhibitory activity was calculated as shown in equation (1):

$$\text{Pancreas lipase inhibitory activity } (\%) = \left[\frac{1 - \left(A_{\text{sample}} - A_{\text{blank}}\right)}{A_{100\%} - A_{0\%}}\right] \times 100, \quad (1)$$

where $A_{sample}$ was the absorbance of sample-lipase-pNPB mixture, $A_{blank}$ was the absorbance of sample-pNPB mixture, $A_{100\%}$ was the absorbance of lipase-pNPB mixture, and $A_{0\%}$ was the absorbance of only pNPB solution.

*2.4. LC-MS Analysis.* 2 mg powder of LGBF was dissolved in 2 mL of 50% acetonitrile and then centrifuged at 16,000 rpm for 5 min to obtain the supernatant for later LC-MS analysis. [14] A Hypersil Gold column (100 × 2.1 mm, 1.9 $\mu$m) was used with the mobile phase (A: 0.1% ($v/v$) formic acid in water; B: acetonitrile) at the following gradient: 0-1 min, 5% B; 1–15 min, 5–100% B; and 15–20 min, 100% B. MS analysis was conducted using an Orbitrap Fusion mass spectrometer (Thermo Fisher Scientific Inc., USA) with the full scan in 100–1500 $m/z$ range.

*2.5. Bioactive Flavonoid Compounds Screening.* Compounds with appropriate pharmacological properties in traditional Chinese medicine seem to be more suitable for design as drugs. Lipinski's rule of five was utilized as the evaluation criteria for screening the potential flavonoid compounds in LGBF, based on the conditions of molecule weight (MW) < 500, number of hydrogen bond donors (Hdon) ≤ 5, number of hydrogen bond acceptors (Hacc) ≤ 10, lipid-water partition coefficient (LogP) ≤ 5, and number of rotatable bonds (Rbon) ≤ 10. [15] The mentioned physicochemical properties of flavonoid compounds identified in LGBF were obtained by the SwissADME online tool (https://www.swissadme.ch/, accessed on 5 January 2023).

*2.6. Compounds and Diabetes-Associated Target Prediction.* The 2D molecular structures of active compounds that satisfied Lipinski's rule of five were downloaded from PubChem (https://pubchem.ncbi.nlm.nih.gov/) and their related target genes were collected via the SwissTargetPrediction database (https://www.swisstargetprediction.ch/). The acknowledged diabetes-related targets were selected from GeneCards (https://www.genecards.org) and the Online Mendelian Inheritance in Man database (https://omim.org/) with the keywords "diabetes" and species "Homo sapiens." Then, a Venn analysis was performed using a web tool (https://bioinfogp.cnb.csic.es/tools/venny/) to find the intersection of compounds- and diabetes-associated targets.

*2.7. Construction of Protein-Protein Interaction (PPI) Network.* To discover the interactions between target proteins, the intersecting targets between compounds and diabetes were imported into the STRING database (https://string-db.org/) with "Homo sapiens" as the species and with a confidence score of ≥0.4. The results from STRING were visually analyzed by Cytoscape 3.7.2 software to perform topology analysis and identify the hub genes.

*2.8. Enrichment Analysis and Compound-Target-Pathway Network Construction.* Gene Ontology (GO) and Kyoto Encyclopedia of Genes and Genomes (KEGG) pathway enrichment analyses were conducted by Metascape (https://metascape.org/) to discover the contributing biological functions and signaling pathways of LGBF in the treatment of diabetes. The GO analysis results, including 10 biological processes (BP), 10 cellular components (CC), 10 molecular functions (MF), and the top 20 KEGG pathways were visualized using an online tool (https://www.bioinformatics.com.cn/). Finally, a "compound-target-pathway" regulatory network was achieved using Cytoscape 3.7.2 software to elucidate the potential antidiabetic mechanisms of LGBF.

*2.9. Molecular Docking Analysis.* To evaluate the binding potential between the compounds and targets, a molecular docking simulation was performed according to the previous report [16]. In brief, the crystal structure of seven flavonoid compounds was downloaded from PubChem databases and optimized by ChemBio3D software. The 3D structure of target proteins was collected via UniProt (https://www.uniprot.org/) and the RCSB-PDB database (https://www.rcsb.org/) followed by the elimination of solvent and organic compounds using PyMol 2.5.2 software. Then, AutoDockTools 1.5.6 was used to conduct molecular docking with format transformation of compounds and target proteins. A docking grid box was constructed to determine its center coordinates and size, and the "number of GA runs" was set to 40. Finally, the visualization of the obtained results was performed by PyMol 2.5.2 software and the Discovery Studio 2019 client software.

*2.10. Animal and Treatment.* C57BL/6J mice (male, 4-5 weeks old) were purchased from Guangzhou Southern Medical University Experimental Animal Technology Development Co., Ltd (Guangzhou, China). All mice were housed in an environment with 25 ± 2°C, 55 ± 10% humidity, 12 h light/dark cycle, and food intake and drink freely. All animal experiments were conducted according to the legislation of the Care and Use of Laboratory Animals issued by the National Institutes of Health and the protocols were approved by the Laboratory Animal Ethics Committee of Southern Medical University on May 13th, 2022 (registration no. L2021084).

After acclimatization for one week, the mice were randomly divided into 2 groups [17]: (1) the blank control group was fed with a normal food diet (4.5 kcal% fat) and (2) the experimental group was fed with HFD (60% kcal fat). Four weeks later, mice in the experimental group were injected with STZ (dissolved in 0.1 M citrate buffer, pH = 4.5) at 40 mg/kg/d (*i.p.*) for 5 consecutive days. The blank control group was injected with 0.1 M citrate buffer only. One week after injection, the fasting blood glucose (FBG) levels of mice were measured via tail vein blood sampling. The T2DM model was considered successfully established when FBG ≥11.1 mM and the FBG value was recorded as the initial level.

The mice were further divided into 6 groups ($n = 8$): (1) the blank control group, which was treated with normal saline by intraperitoneal injection; (2) the model group, which was treated with normal saline by intraperitoneal

injection; (3) the positive control group, which was treated with metformin as a positive drug at 80 mg/kg/d by intraperitoneal injection; (4) the LGBF-70 group, which was treated with LGBF at 70 mg/kg/d by intraperitoneal injection; (5) the LGBF-35 group, which was treated with LGBF at 35 mg/kg/d by intraperitoneal injection; and (6) the LGBF-17.5 group, which was treated with LGBF at 17.5 mg/kg/d by intraperitoneal injection. The body weight and food intake were recorded every week. 28 days later, the mice were anesthetized with pentobarbital sodium and executed by cervical dislocation. The blood samples were collected from the eyeball and FBG was detected. The liver tissues were obtained, washed, and weighed. The liver index was calculated as shown in equation (2):

$$\text{Liver index} = \frac{\text{Liver weight } (g)}{\text{Body weight } (g)}. \quad (2)$$

*2.11. Oral Glucose Tolerance Test (OGTT).* On the 14th day of administration, all mice were fasted for 6 h. The tail vein blood was collected and the fasting blood glucose was recorded as the initial blood glucose (0 min). Subsequently, the mice were orally administrated with 2 g/kg of glucose, and the blood glucose levels were measured at 30, 60, and 120 min, respectively. Then, the blood glucose change curve was constituted and the area under the curve (AUC) was used as an indicator of the glucose tolerance ability. Higher AUC represented worse glucose tolerance ability.

*2.12. Insulin Tolerance Test (ITT).* On the 25th day of administration, all mice were fasted for 6 h. Then, the mice were given 0.5 U/kg of insulin by intraperitoneal injection. The AUC of the curve was used as an indicator to determine the insulin tolerance ability and a higher AUC represented worse insulin tolerance ability.

*2.13. Biochemical Analysis.* The blood samples were centrifuged at 4000 rpm at 4°C for 10 min to isolate the serum. The fasting insulin, TG, and TC levels in the serum of mice were detected using the commercially available kits strictly based on the manufacturers' instructions. The homeostatic model assessment of insulin resistance (HOMA-IR) was calculated based on equation (3):

$$\text{HOMA} - \text{IR} = \text{FBG} \times \frac{\text{fasting insulin level}}{22.5}. \quad (3)$$

Furthermore, the circulating levels of high-density lipoprotein cholesterol (HDL-C), aspartate transaminase (AST), and alanine transaminase (ALT) were evaluated via the Mindray BS-33OE master instrument.

*2.14. Hematoxylin-Eosin Staining.* After being fixed in 4% paraformaldehyde at 4°C, the liver was dehydrated by a gradient of ethanol solutions and embedded in paraffin. Then, the liver sections were cut into 4 $\mu$m and stained with hematoxylin and eosin. After drying, the sections were observed and photographed by a pathology section scanner.

*2.15. Western Blot Analysis.* The liver stored at −80°C was used to extract the total protein. After determining the protein concentration with a BCA protein assay kit (Thermo Fisher Scientific, Waltham, MA, USA), the total protein was adjusted to the appropriate concentration and protein denaturation was achieved by heating at 100°C for 10 min. Subsequently, the resulting solution was used for Western blot analysis on the 10% SDS-PAGE and transferred to PVDF membranes (Millipore, Billerica, MA, USA). After transformation, the protein bands were split according to the molecular weight of the corresponding protein and blocked in a 5% skim milk powder solution for 75 min. Then, the protein blanks were washed 3 times with TBST solution, followed by primary antibodies and secondary antibodies incubation. Finally, the protein blanks were visualized by ECL and the chemiluminescence detection system (Bio-Rad, CA, USA).

*2.16. Statistical Analysis.* GraphPad Prism 7.0 software (San Diego, CA, USA) was used for data analyses, and the results were shown as the mean ± standard deviation (SD). The difference among 3 or more groups was analyzed with one-way ANOVA; and student's *t*-test was used for 2 parametric groups. The bands of Western blot proteins were evaluated by Image-J software. It was considered statistically significant when the $P$ value was $<0.05$.

## 3. Results

*3.1. Pancreas Lipase Assay.* As shown in Figure 1, different fractions extracted from leaves of *L. gracile* exhibited different regulation on the pancreas lipase activity. In brief, the 30% ethanol fractions at 0.5–4 mg/mL presented an increasing tendency toward the pancreas lipase activity. 90% ethanol fractions at lower concentrations of 0.25–1 mg/mL significantly inhibited the pancreas lipase activity, while those at 2–4 mg/mL showed stimulatory effects. Both 50% and 70% ethanol fractions markedly blocked the pancreas lipase activity, whose inhibition rate at 0.25–2 mg/mL was nearly close to that of the positive orlistat group.

The total flavonoid contents of 50% and 70% ethanol fractions were determined to be 31.19% and 22.63%, respectively. Hence, 50% ethanol fractions with a higher flavonoid content and great pancreas lipase inhibitory activity were recognized as LGBF and employed for further investigation.

*3.2. Flavonoid Compounds Identified in LGBF.* A total of twelve flavonoid compounds, including diosmetin 7-O-beta-D-glucopyranoside, puerarin, naringin, diosmin, neohesperidin, hesperetin, isosinensetin, sinensetin, 6-demethoxytangeretin, nobiletin, tangeretin, and demethylnobiletin, were identified in LGBF. The chemical structures are shown in Figure 2. These flavonoid compounds were further analyzed for their suitability in drug application according to Lipinski's rule of five. The results of SwissADME prediction showed that seven compounds including hesperetin, isosinensetin, sinensetin, 6-demethoxytangeretin, nobiletin,

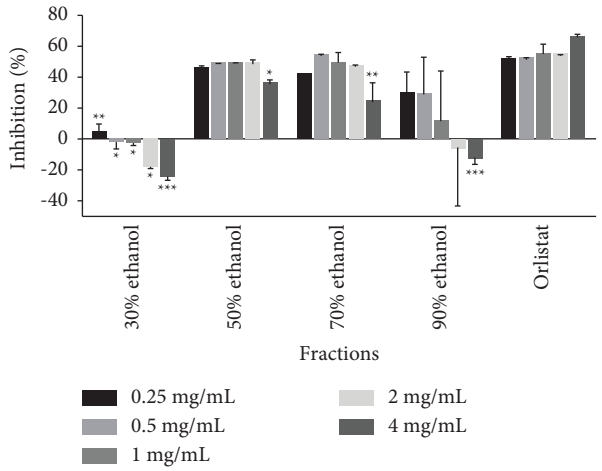


Figure 1: Pancreas lipase inhibitory activity of 30%, 50%, 70%, and 90% ethanol fractions from leaves of *L. gracile*. $^{*}P < 0.05$, $^{**}P < 0.01$, and $^{***}P < 0.001$ versus the positive group.

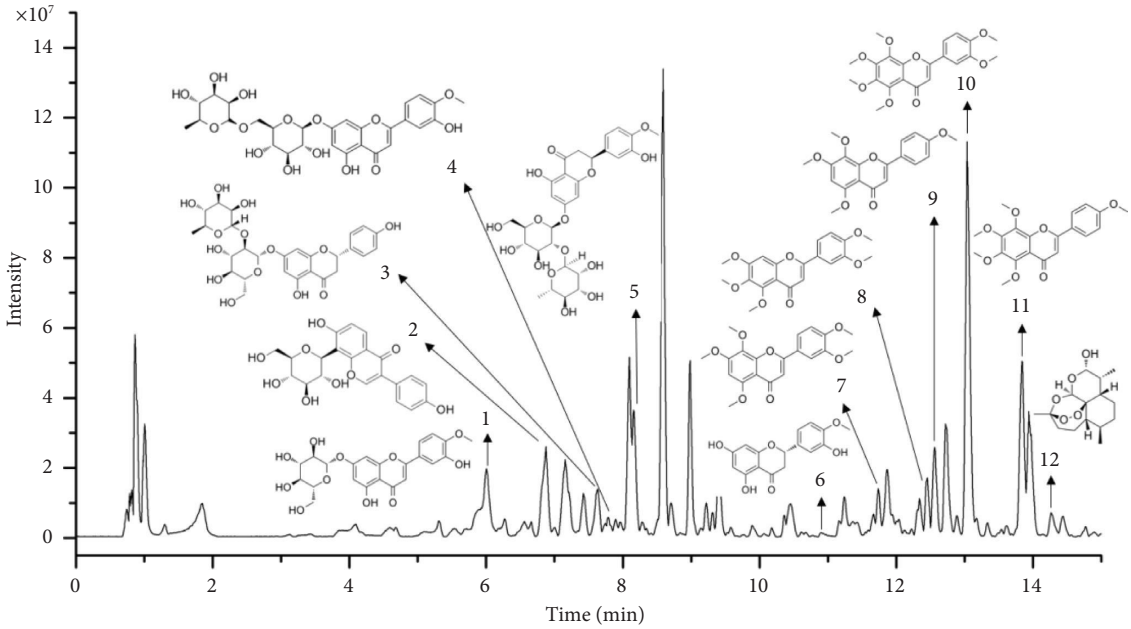


Figure 2: LC-MS profiles of LGBF and the chemical structures of identified compounds: peaks of 1–12 represent diosmetin 7-O-beta-D-glucopyranoside, puerarin, naringin, diosmin, neohesperidin, hesperetin, isosinensetin, sinensetin, 6-demethoxytangeretin, nobiletin, tangeretin, and demethylnobiletin, respectively.

tangeretin, and demethylnobiletin conformed to Lipinski's rule of five [18–22]. More details about LC-MS analysis and the pharmacological properties are demonstrated in Table 1. Hence, hesperetin, isosinensetin, sinensetin, 6-demethoxytangeretin, nobiletin, tangeretin and demethylnobiletin were considered as seven potential flavonoid compounds of LGBF, which were employed for further studies.

*3.3. Diabetes-Related Targets.* After the deletion of duplicates, a total of 201 target genes related to seven potential flavonoid compounds of LGBF and 17701 diabetes-associated targets were collected. Moreover, the Venn analysis showed that 189 intersecting targets were discerned from the compound and diabetes-associated targets, which were considered as potential therapeutic targets of LGBF against diabetes (Figure 3(a)).

*3.4. PPI Network and Core Targets.* The PPI information of intersecting target genes was exported from the STRING database and then a PPI network consisting of 189 nodes and 1426 edges was established by Cytoscape (Figure 3(b)). Based on topological analysis, the targets that occupied the core position in the network were considered as the key antidiabetic targets of LGBF. As shown in Figure 3(c), the top 10 targets with the highest degree values were identified as AKT1 (93), SRC (73), EGFR (67), ESR1 (67), CCND1 (56), PTGS2 (55), PPARG (50), MMP9 (48), AR (43), and PIK3CA (41).

Table 1: Chemical compounds identified in LGBF and their pharmacological properties.

| No. | Compounds | Molecular formula | RT (min) | CAS | MW (g/mol) | Rbon | Hacc | Hdon | LogP |
|---|---|---|---|---|---|---|---|---|---|
| 1 | Diosmetin 7-O-beta-D-glucopyranoside | $C_{22}H_{22}O_{11}$ | 6.00 | 20126-59-4 | 462.4 | 5 | 11 | 6 | 0.57 |
| 2 | Puerarin | $C_{21}H_{20}O_9$ | 6.87 | 3681-99-0 | 416.38 | 3 | 9 | 6 | 0.23 |
| 3 | Naringin | $C_{27}H_{32}O_{14}$ | 7.62 | 10236-47-2 | 580.53 | 6 | 14 | 8 | −0.87 |
| 4 | Diosmin | $C_{28}H_{32}O_{15}$ | 7.82 | 520-27-4 | 608.54 | 7 | 15 | 8 | −0.52 |
| 5 | Neohesperidin | $C_{28}H_{34}O_{15}$ | 8.16 | 13241-33-3 | 610.56 | 7 | 15 | 8 | −1.02 |
| 6 | Hesperetin | $C_{16}H_{14}O_6$ | 10.90 | 520-33-2 | 302.28 | 2 | 6 | 3 | 1.91 |
| 7 | Isosinensetin | $C_{20}H_{20}O_7$ | 11.74 | 17290-70-9 | 372.37 | 6 | 7 | 0 | 2.98 |
| 8 | Sinensetin | $C_{20}H_{20}O_7$ | 12.34 | 2306-27-6 | 372.37 | 6 | 7 | 0 | 3.1 |
| 9 | 6-demethoxytangeretin | $C_{19}H_{18}O_6$ | 12.56 | 6601-66-7 | 342.34 | 5 | 6 | 0 | 3 |
| 10 | Nobiletin | $C_{21}H_{22}O_8$ | 13.04 | 478-01-3 | 402.39 | 7 | 8 | 0 | 3.02 |
| 11 | Tangeretin | $C_{20}H_{20}O_7$ | 13.84 | 481-53-8 | 372.37 | 6 | 7 | 0 | 3.02 |
| 12 | Demethylnobiletin | $C_{20}H_{20}O_8$ | 14.27 | 2174-59-6 | 388.37 | 6 | 8 | 1 | 2.78 |

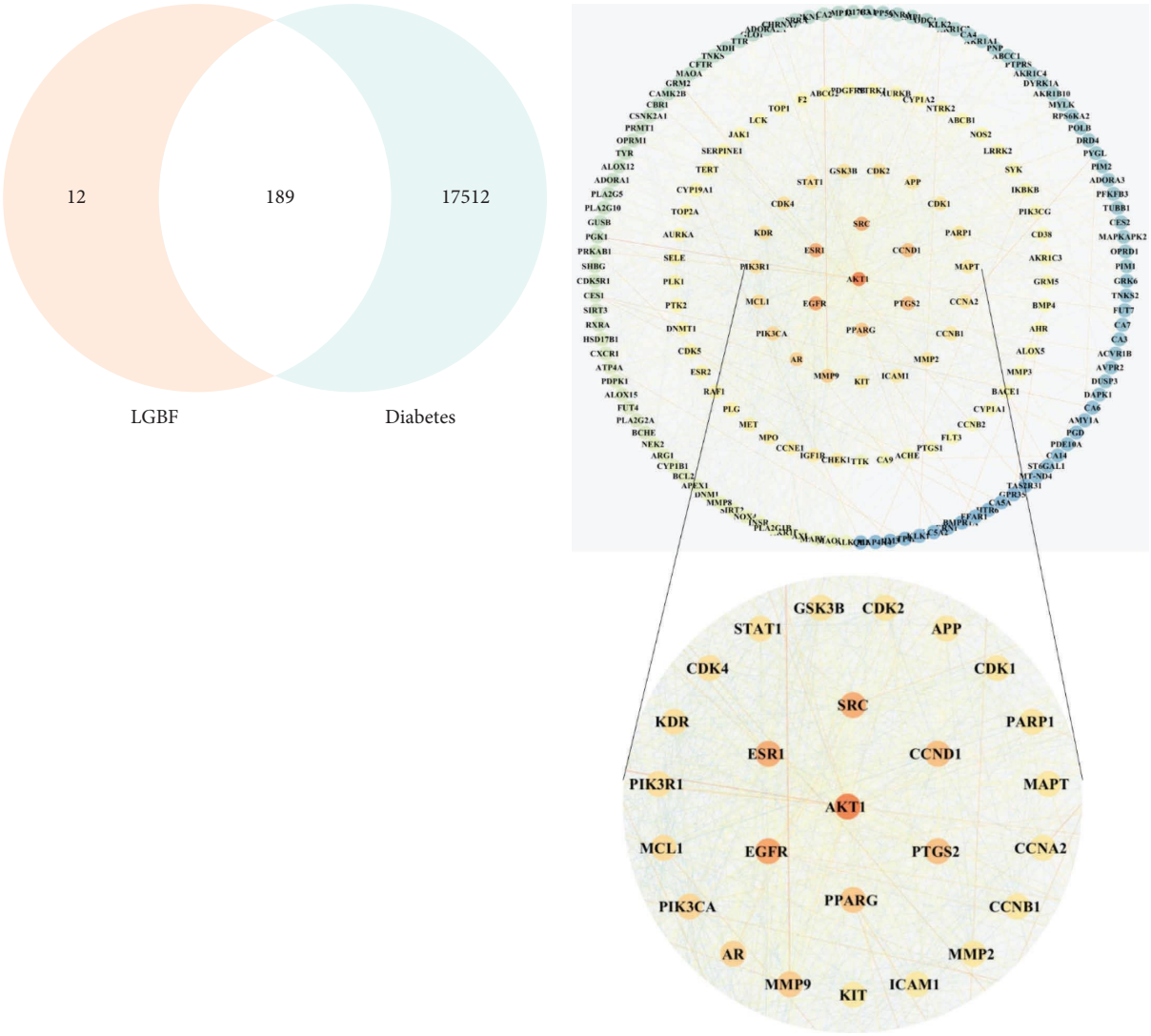


(a) (b)

Figure 3: Continued.

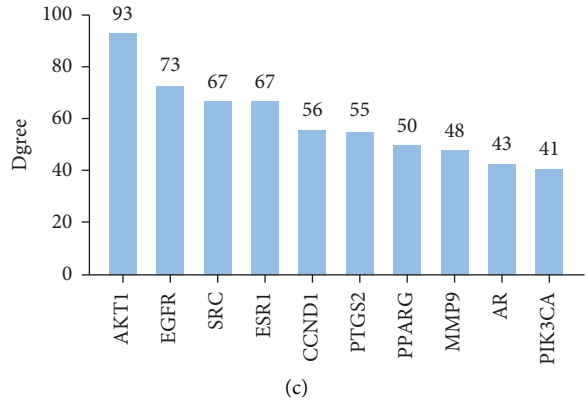


Figure 3: Construction of the PPI network and identification of core targets: (a) Venn diagram of the intersecting targets between LGBF and diabetes, (b) PPI network of the 189 potential therapeutic targets, and (c) the 10 core targets with the highest degree of the PPI network.

*3.5. GO and KEGG Pathway Enrichment Analyses.* To elucidate the biological role of LGBF, GO enrichment analysis was conducted by Metascape, resulting in a total of 1615 BP, 115 CC, and 193 MF. Figure 4(a) shows the top 10 BP, CC, and MF, which were primarily involved in lipid metabolism, inflammatory response, and protein transport. Specifically, BP terms indicated that LGBF exerted therapeutic effects on diabetes mainly through protein phosphorylation, cellular response to nitrogen compounds, and peptidyl-serine phosphorylation. Moreover, 179 signaling pathways were obtained by KEGG enrichment analysis, and the top 20 are illustrated in Figure 4(b). It was suggested that the potential targets of LGBF were highly correlated with PI3K/AKT and NF-$\kappa$B signaling pathways. The PI3K/AKT pathway is a classic pathway associated with diabetes, which plays a critical role in regulating glucose transport. The NF-$\kappa$B signaling pathway is also proven to be closely involved in diabetes-related inflammation.

*3.6. Compound-Target-Pathway Network Analysis.* As illustrated in Figure 5, a compound-target-pathway network with 70 nodes was used to display the intricate interactions among seven compounds, 58 intersecting targets, and 10 key pathways, indicating that LGBF might act on multiple targets and pathways owing to its multiple compounds. According to the topological analysis, 5 targets including AKT1, EGFR, IGF1R, CDK2, and MET participated in the top 5 KEGG enrichment pathways with a high frequency. Especially, AKT1 and EGFR were core targets identified in PPI analysis and enriched in the PI3K/AKT pathway.

*3.7. Molecular Docking Results.* Molecular docking validation was applied to analyze the possibility of interaction between the seven active ingredients and 10 core targets. The docking score was used to evaluate the binding energy and a score of $<-5.0$ kcal/mol represented a good binding affinity. As shown in Figure 6(a), most targets had a low binding energy, indicating the relatively stable binding with the compounds of LGBF. Particularly, the scores of PIK3CA ($-8.04$ kcal/mol) and AKT1 ($-6.26$ kcal/mol) with all compounds were less than $-5.0$, suggesting that LGBF could have good interactions with PIK3CA and AKT1. Moreover, each target with the lowest score was visualized to show the hydrogen bonding and active site (Figures 6(b)–6(i)). It was observed that compact complexes were formed between the components and target genes. These results suggested that the bioactive flavonoid compounds from LGBF could combine with the core target receptors, thus exerting antidiabetic effects.

*3.8. LGBF Treatment Modulated Body Weight, Food Intake, and Liver Index.* During the 4 weeks of administration, the body weight of mice in the model group increased significantly tardily, compared with that in the normal blank group (Figure 7(a)). However, LGBF and the positive control metformin intervention exhibited a decreasing tendency toward body weight gain (Figure 7(b)). It was also found that LGBF administration at 35 mg/kg significantly inhibited HFD and STZ-induced increases in the liver index (Figure 7(c)).

*3.9. LGBF Treatment Ameliorated Insulin Resistance.* As depicted in Figure 7(d), mice in the model group showed significantly impaired glucose tolerance compared with the normal mice in the blank group. In contrast, LGBF administration at 35 and 70 mg/kg potently recovered glucose tolerance, as evidenced by the decreased AUC levels (Figure 7(e)). Similar results were presented in the ITT, which showed that LGBF treatment significantly improved the insulin tolerance of HFD and STZ-induced mice (Figures 7(f) and 7(g)). Notably, Figure 7(h) reveals that the insulin contents in T2DM mice were slightly reduced only; however, the LGBF intervention showed a potential tendency to increase the serum insulin levels. Figure 7(i) shows that 28 days of administration of LGBF at 35 and 70 mg/kg effectively inhibited the FBG levels, as compared with the model group. However, LGBF administration dose-dependently reduced the HOMA-IR index (Figure 7(j)). These data evidenced that LGBF administration probably increased the insulin sensitivity of diabetic mice.


Figure 4: GO and KEGG pathway enrichment analyses of 189 intersecting targets: (a) the top 10 BP, MF, and CC of GO enrichment analysis and (b) the top 20 pathways of KEGG pathway enrichment analysis.

*3.10. LGBF Treatment Regulated Lipid Profiles and AST/ALT Ratio in Liver.* As shown in Figure 8(a), a significant difference in HDL-C levels in the serum of mice was observed in the blank and model groups. Nevertheless, LGBF administration at 35 and 70 mg/kg markedly reduced the elevated HDL-C levels by HFD and STZ treatment. Specifically, when mice were supplemented with LGBF at 35 mg/kg, the HDL-C level was decreased to $2.127 \pm 0.2444$ mM, much lower than that in the DM mice ($3.62 \pm 0.1744$ mM). LGBF addition at 35 and 70 mg/kg also showed a greater potency than metformin in inhibiting TC levels (Figure 8(b)). Moreover, HFD and STZ-induced increases in TG levels were significantly decreased by LGBF intervention at 17.5, 35, and 70 mg/kg (Figure 8(c)). In

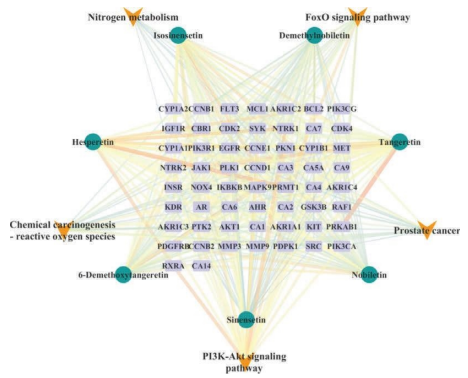


Figure 5: Construction of compound-target-pathway network: the yellow nodes represent the target of LGBF for diabetes, the green nodes represented the active flavonoid compounds identified in LGBF, and the red nodes represent the top 5 KEGG enrichment pathways.

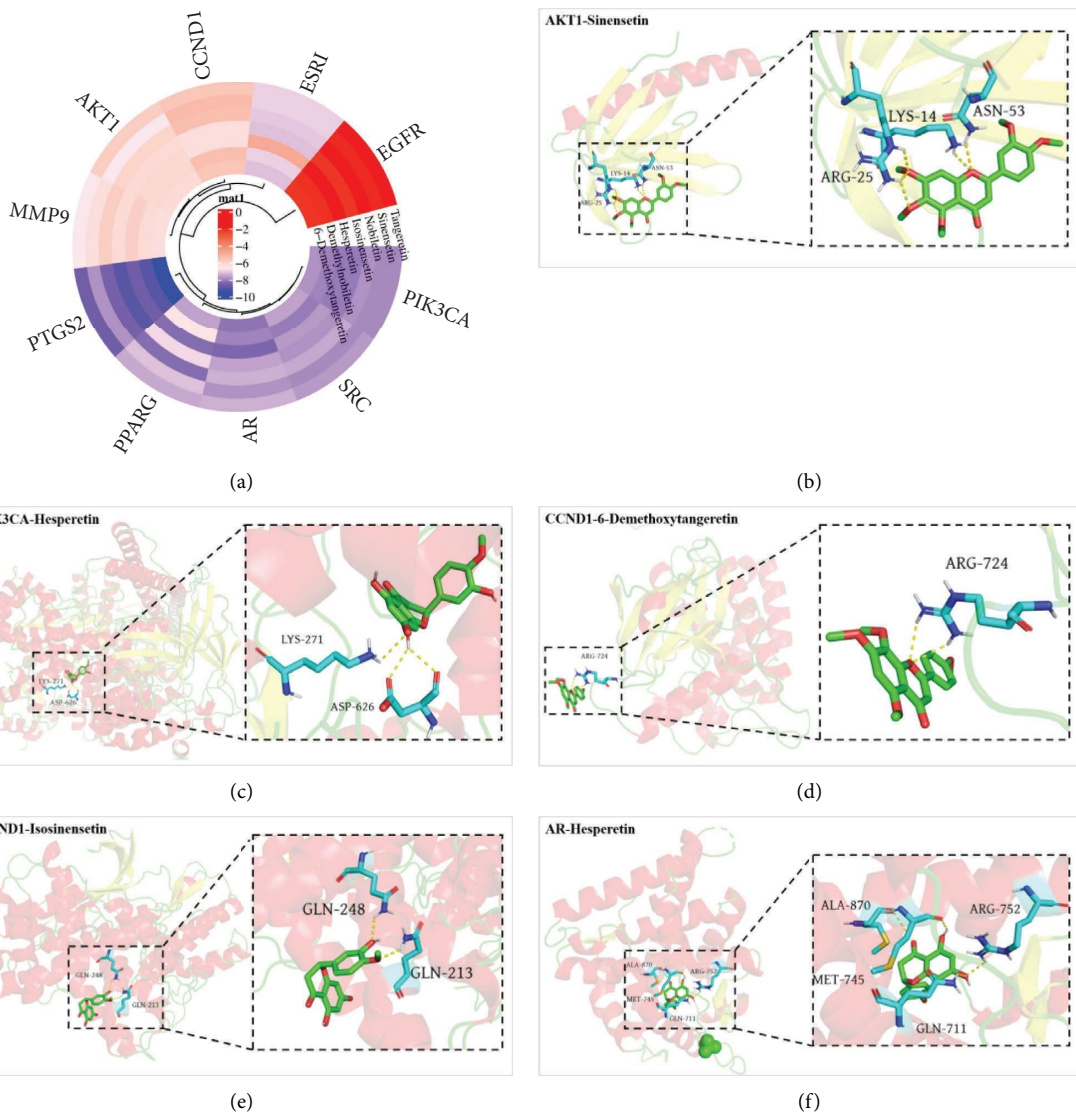


Figure 6: Continued.

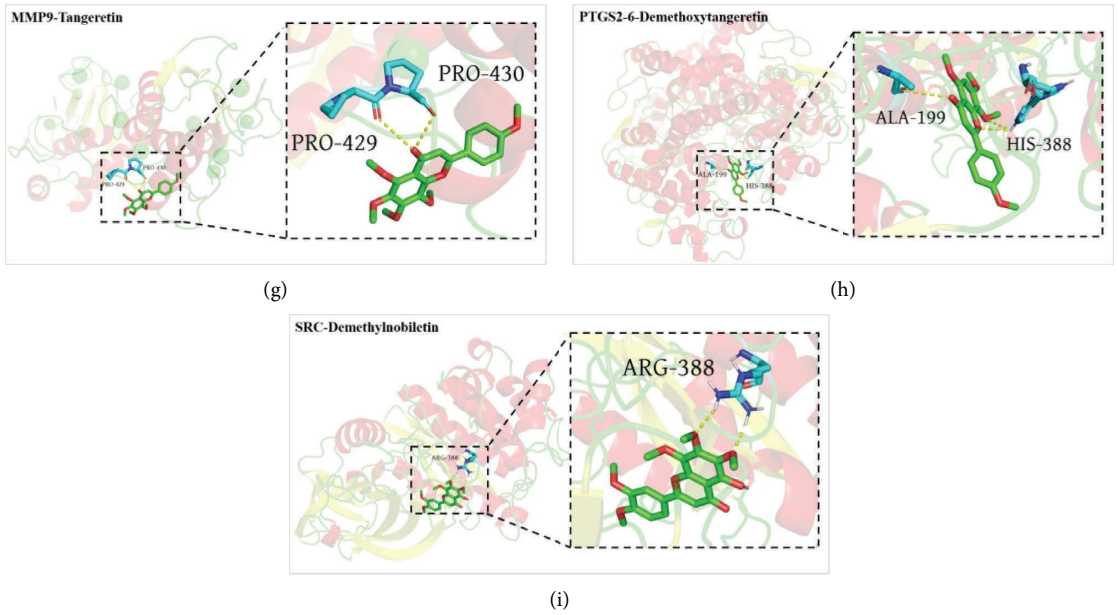


Figure 6: Molecular docking analysis of LGBF: (a) circular heatmap of binding energy between compounds and targets and (b–i) 3D binding diagrams of each target with the lowest score. The compounds are shown as green rods, the active sites are displayed as blue rods, and they are connected by yellow hydrogen bonds.

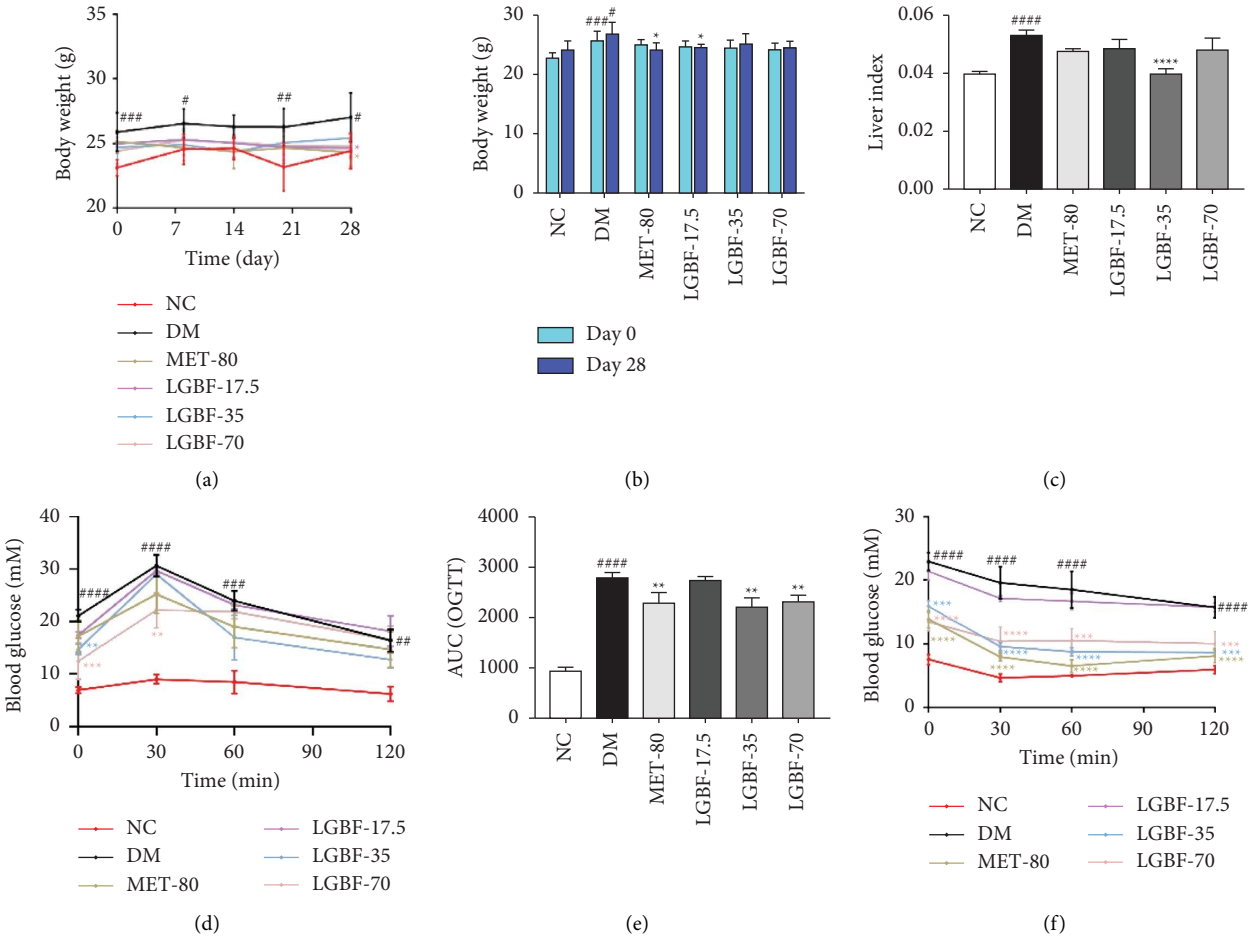


Figure 7: Continued.

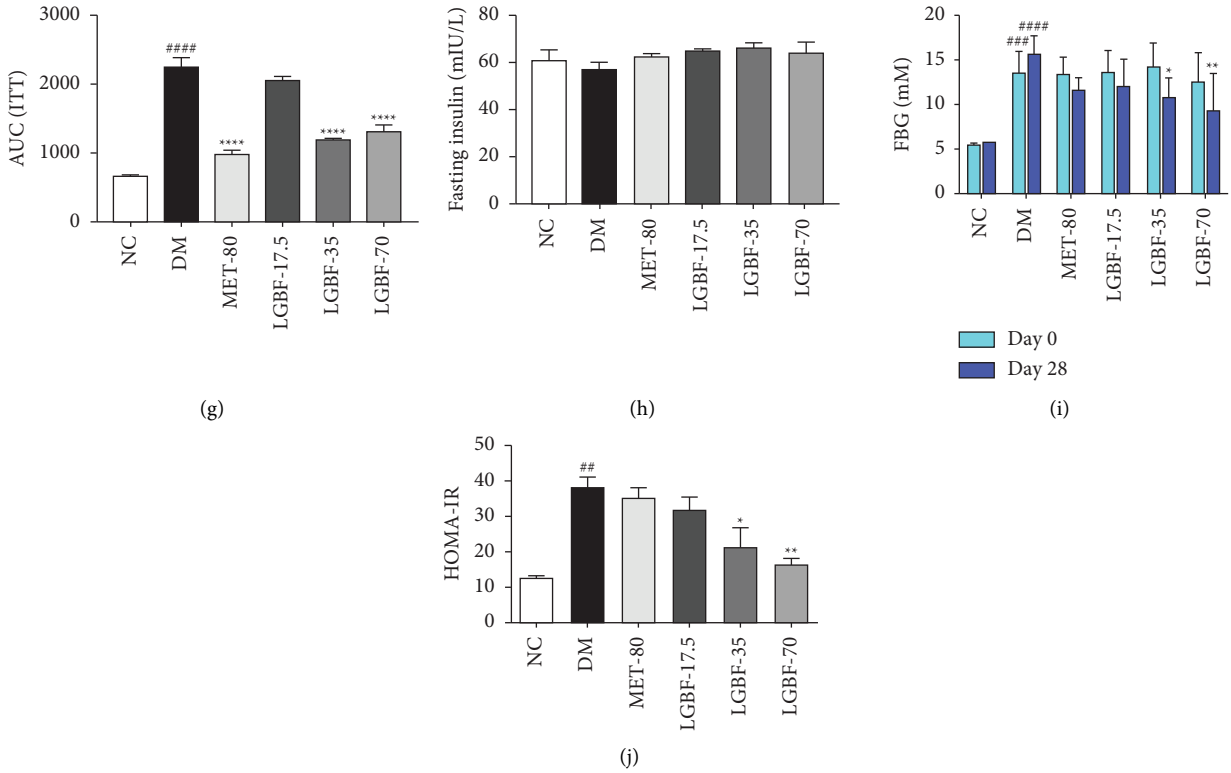


Figure 7: Effects of LGBF on insulin resistance in HFD and STZ-induced diabetic mice: (a) body weight changes each week, (b) body weight changes before and after administration, (c) liver index, (d) the blood glucose changes curve of OGTT, (e) AUC of the OGTT blood glucose change curve, (f) the blood glucose changes curve of ITT, (g) AUC of the ITT blood glucose change curve, (h) fasting insulin level in serum, (i) FBG before and after administration, and (j) HOMA-IR index. All experiments were repeated at least 3 times. The results are shown as mean ± SD. $^{\#}P < 0.05$, $^{\#\#}P < 0.01$, $^{\#\#\#}P < 0.001$, and $^{\#\#\#\#}P < 0.0001$ versus the blank group. $^{*}P < 0.05$, $^{**}P < 0.01$, $^{***}P < 0.001$, and $^{****}P < 0.0001$ versus the model group.

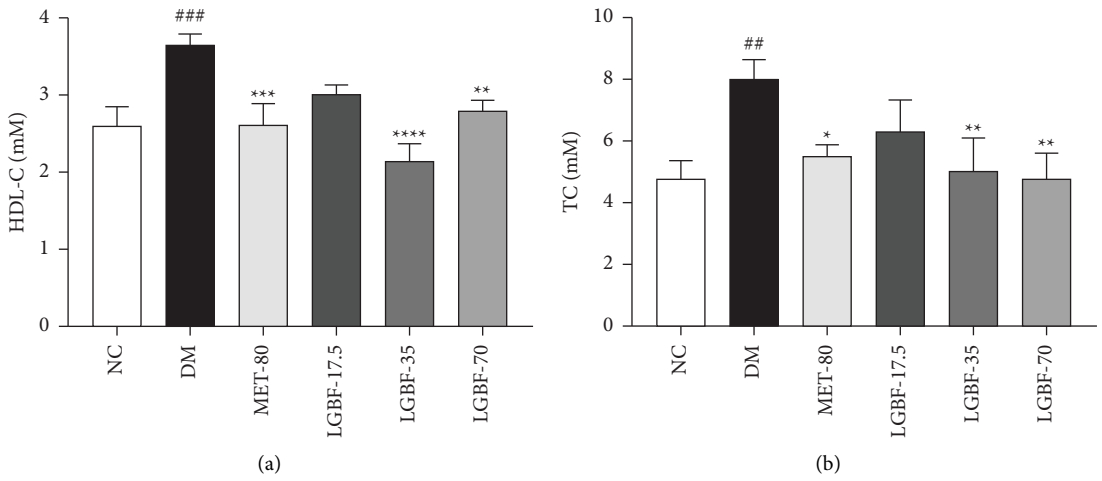


Figure 8: Continued.

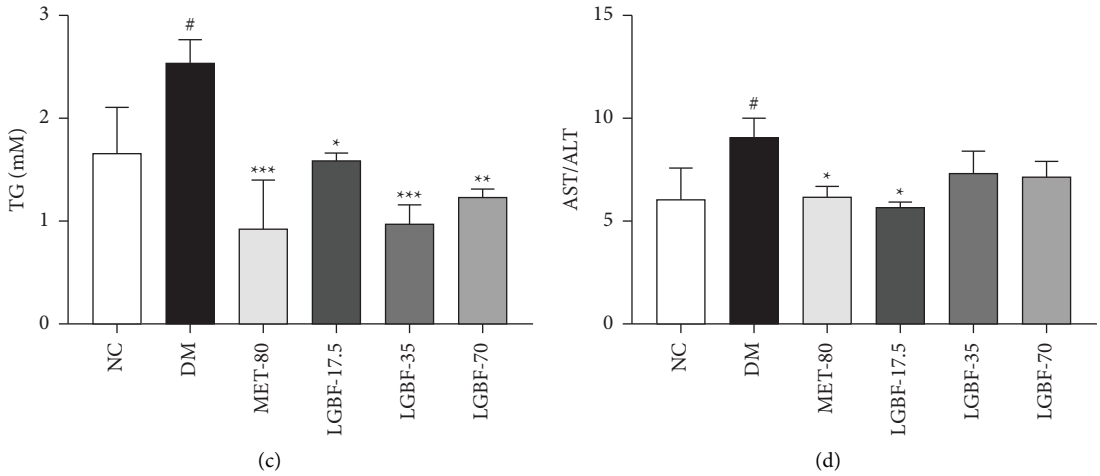


Figure 8: Effects of LGBF on serum lipid profiles and AST/ALT ratio in HFD and STZ-induced diabetic mice: (a) HDL-C, (b) TC, (c) TG, and (d) AST/ALT ratio. All experiments were repeated at least 3 times. The results are shown as mean ± SD. $^{\#}P < 0.05$, $^{\#\#}P < 0.01$, $^{\#\#\#}P < 0.001$, and $^{\#\#\#\#}P < 0.0001$ versus the blank group. $^{*}P < 0.05$, $^{**}P < 0.01$, $^{***}P < 0.001$, and $^{****}P < 0.0001$ versus the model group.

addition, LGBF intervention at the minimum concentration of 17.5 mg/kg significantly recovered the AST/ALT ratio back to normal levels, suggesting the protective potential of LGBF against HFD and STZ-induced liver dysfunction (Figure 8(d)). These data indicated that LGBF treatment contributed to the improvement of serum lipid profiles and liver functions.

*3.11. LGBF Treatment Altered Histopathological Changes in Liver.* Macroscopical photographs of livers and hematoxylin and eosin staining of the liver were obtained to characterize the effects of LGBF on hepatic histopathology. As macroscopically shown in Figure 9, yellow fatty-like masses of tissue were visible on the liver surface of the DM mice treated with LGBF at the lowest dose, which were particularly evident in the model control group. It demonstrated that chronic HFD-fed induced lipid accumulation in the liver. The results of hematoxylin and eosin staining clearly signaled that the liver of normal control mice showed normal morphology and structure, while inflammation (lighter color of cytoplasm) and intracellular lipid accumulation (hollows with regular edges and deformed cell morphology) were observed in HFD and STZ-induced mice. As expected, LGBF treatment at 35 and 70 mg/kg potently attenuated the inflammation and lipid accumulation in the liver of the diabetic mice. The efficacy of LGBF intervention at 35 mg/kg was comparable to that of the positive control metformin. These facts indicated that LGBF administration probably significantly alleviated hepatic histopathology in diabetic mice.

*3.12. LGBF Treatment Activated the PI3K/AKT Pathway.* The expression of p-AKT and p-PI3K protein are shown in Figures 10(a)–10(c). HFD combined with STZ sharply decreased the expression of p-AKT and p-PI3K, whereas LGBF treatment markedly reversed this condition, with 17.5 mg/kg being more effective. These data indicated that LGBF might mitigate the liver damage in diabetic mice by activating the PI3K/AKT pathway.

*3.13. LGBF Treatment Inhibited NF-κB Activation.* HFD and STZ supplementation led to significant increases in IL-1$\beta$ expression levels, suggesting that the inflammatory responses occurred in the diabetic mice. However, 4 weeks of administration of LGBF at 17.5, 35, and 70 mg/kg dramatically reversed IL-1$\beta$ expression to normal levels. Further data evidenced that the anti-inflammatory activities of LGBF were probably related to the NF-κB pathway. Of note, the expression levels of p-P65 in the liver of mice were significantly and dose-dependently reduced from 0.9015 to 0.1835, 0.2085, and 0.418, respectively, when treated with LGBF at 17.5, 35, and 70 mg/kg (Figures 10(d)–10(f)).

## 4. Discussion

With the epidemic of T2DM, searching for novel medicines for the treatment of T2DM and its associated disorders has attracted great attention recently [23]. *L. gracile* leaves have been popularly consumed in China as folk medicine and dietary supplements [9]. Nevertheless, the effects of flavonoids from *L. gracile* leaves on T2DM and the possible mechanisms need further studies. In the current study, the hypoglycemic and lipid-lowering effects of LGBF on HFD-STZ-induced T2DM mice were confirmed. LGBF-treated mice showed improved lipid profiles, insulin sensitivity, and hepatic histopathology, as well as reduced hepatic inflammation.

LC-MS analysis showed that twelve flavonoid compounds were identified from LGBF and seven compounds that satisfied Lipinski's rule of five were selected for further research. Among them, isosinensetin, hesperetin, sinensetin, nobiletin, and tangeretin were reported to exert significant protective effects against diabetes-related diseases in various models. For example, isosinensetin could increase glucagon-like peptide 1 by activating human bitter taste receptor

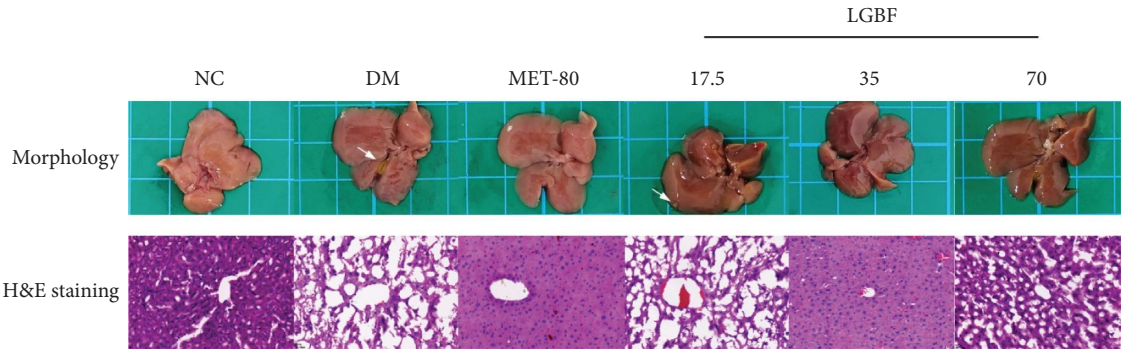


Figure 9: Effects of LGBF on histopathological alternations in the liver of HFD and STZ-induced diabetic mice by morphology photos and hematoxylin and eosin staining at 400x magnification.

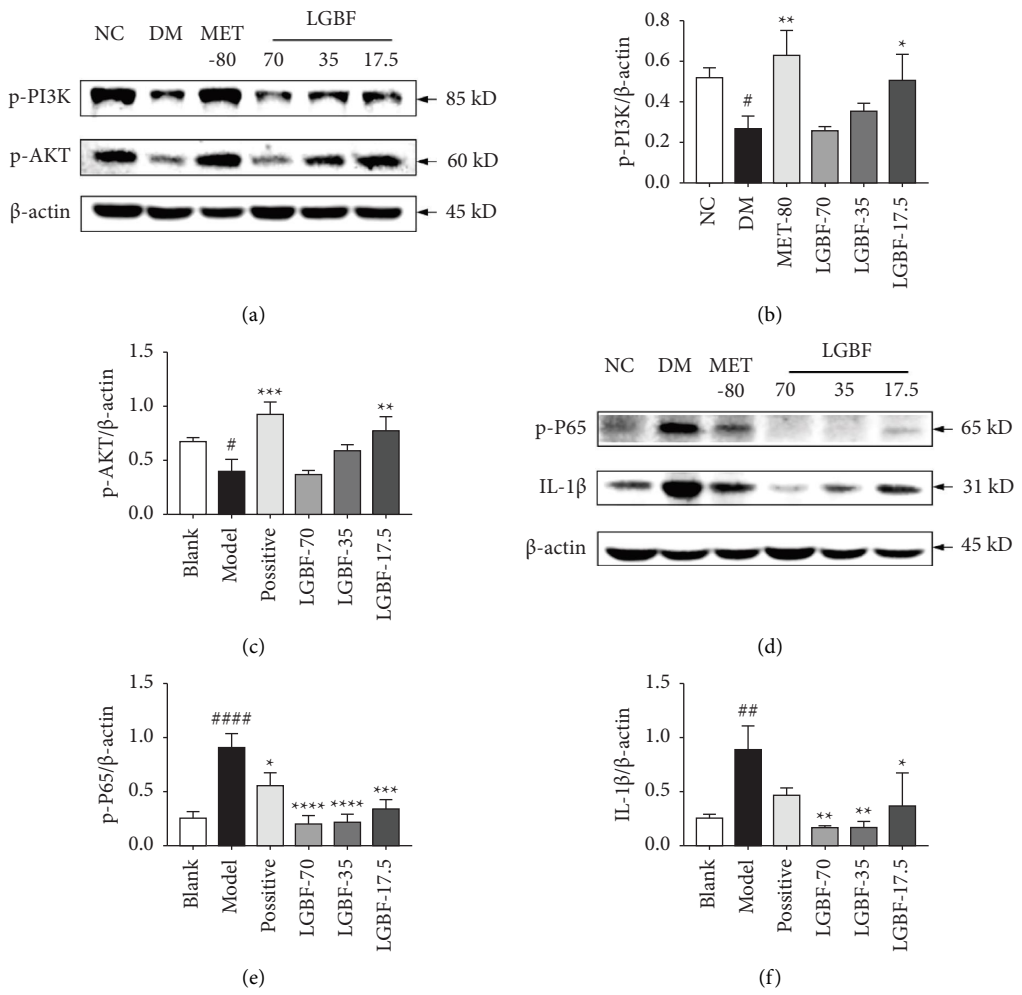


Figure 10: Effects of LGBF on the PI3K/AKT pathway and inflammation suppression in HFD and STZ-induced diabetic mice: (a) representative Western blot images of p-PI3K and p-AKT, (b) expression levels of p-PI3K with respect to $\beta$-actin, (c) expression levels of p-AKT with respect to $\beta$-actin, (d) representative Western blot images of p-P65 and IL-1$\beta$, (e) expression levels of p-P65 with respect to $\beta$-actin, and (f) expression levels of IL-1$\beta$ with respect to $\beta$-actin. All experiments were repeated at least 3 times. The results are shown as mean ± SD. $^{\#}P < 0.05$, $^{\#\#}P < 0.01$, $^{\#\#\#}P < 0.001$, and $^{\#\#\#\#}P < 0.0001$ versus the blank group. $^{*}P < 0.05$, $^{**}P < 0.01$, $^{***}P < 0.001$, and $^{****}P < 0.0001$ versus the model group.

subtype 50 and gbetagamma-mediated pathway in NCI-H716 cells [19]. Hesperetin attenuated T2DM in rats by altering insulin receptor/PI3K and AMPK pathways [18]. Nobiletin provided hypoglycemic protection in STZ-challenged mice via the regulation of islet beta-cell mitophagy and gut microbiota homeostasis [22].

Sinensetin and tangeretin were also promising agents for treating diabetes [20, 21]. Therefore, LGBF containing these potential antidiabetic compounds might show predominant capacities against diabetes-related diseases via diverse mechanisms acting simultaneously.

Network pharmacology analysis demonstrated that the core targets of LGBF against diabetes were AKT1, SRC, EGFR, ESR1, CCND1, PTGS2, PPARG, MMP9, AR, and PIK3CA, which were mainly involved in lipid metabolism and inflammatory responses. Specifically, AKT1 and PIK3CA are typical elements in the PI3K-AKT signaling pathway, participating in various biological processes in cells such as proliferation, differentiation, apoptosis, and glucose transport [24]. GO and KEGG enrichment analyses further revealed that the PI3K/AKT pathway was predicted as the most important signaling pathway of LGBF against diabetes. The PI3K/AKT pathway is a primary insulin receptor signaling pathway, which mainly regulates energy metabolism, and the notion that the liver is the main metabolic organ directly affecting the lipid mass spectrum is widely acknowledged [25, 26]. Besides, emerging views have considered that the PI3K/AKT signaling pathway plays a vital role in inflammation regulation, especially the chronic liver disease by adjusting the polarization of macrophages [27]. A growing number of studies have expounded on how the PI3K/AKT pathway regulates liver functions in T2DM after medication or surgery intervention. For example, both sleeve gastrectomy and $\gamma$-glutamylcysteine intervention could ameliorate T2DM-induced hepatic injuries through this pathway [28, 29]. In this present study, it was noted that the expression of p-PI3K and p-AKT in the liver were significantly increased when mice were administrated with LGBF at 17.5 mg/kg for 4 weeks, indicating the positive effects of LGBF on liver metabolism.

Diabetes has become a normalized complication of incident hepatic diseases, particularly in obese individuals [30]. Owing to HFD-induced abnormal lipid metabolism, the concentration of lipid droplets is beyond the capability of adipocytes. When the lipid from adipose tissue ectopically accumulates in the liver, macrophage infiltration increases and hepatic inflammation occurs [31]. The release of inflammatory factors blocks the insulin signaling, including the PI3K/AKT pathway, and results in impaired glucose metabolism or even hyperglycemia. Interestingly, the activation of the PI3K/AKT pathway not only improves energy metabolism but also facilitates M2-type macrophage polarization, promoting anti-inflammatory reactions [32]. To further explore the affect caused by LGBF on the interaction between PI3K/AKT signaling and hepatic inflammation, this study was interested in testing whether LGBF intervention suppressed the inflammatory responses in the liver. As expected, LGBF addition markedly decreased HFD and STZ-induced increases of IL-1$\beta$ expression in the liver, which was a crucial proinflammatory cytokine that affects insulin sensitivity and induces T2DM [33]. This fact implied that LGBF probably played a role in inhibiting hepatic inflammation. Thus, further assays were performed to explore the effects of LGBF on the NF-$\kappa$B pathway, a classical inflammatory signaling pathway in response to various injuries and infections. For example, numerous studies have demonstrated that sodium salicylate, a classical anti-inflammatory drug, can ameliorate T2DM via the NF-$\kappa$B pathway inhibition [33]. The data evidenced that LGBF treatment potently inhibited p-P65 phosphorylation at lower concentrations. Hence, LGBF might alleviate hepatic inflammation in T2DM by inhibiting NF-$\kappa$B activation.

## 5. Conclusions

In the present study, seven crucial flavonoid compounds of LGBF related to diabetes were screened by LC-MS and the network pharmacology analysis, including hesperetin, isosinensetin, sinensetin, 6-demethoxytangeretin, nobiletin, tangeretin, and demethylnobiletin. Furthermore, a compound-target-pathway construction was established, revealing the involvement of 58 targets and 10 pathways, especially the PI3K/AKT pathway. More importantly, it was found that LGBF administration significantly improved the lipid profiles and insulin sensitivity in HFD and STZ-induced diabetic mice. Additionally, LGBF demonstrated its role in the regulation of key protein expression within the PI3K/AKT and NF-$\kappa$B pathways, thereby markedly ameliorating liver injuries in diabetic mice through the regulation of hepatic metabolism and inflammation. In summary, LGBF is a viable functional food component for diabetes medication development.

## Abbreviations

T2DM: Type 2 diabetes mellitus
*L*. Brongn: *Lophatherum gracile* Brongn
LGBF: Flavonoids from *L*. Brongn leaves
IR: Insulin resistance
NF-$\kappa$B: Nuclear factor-kappa B
IL-1$\beta$: Interleukin-1$\beta$
PI3K: Phosphatidylinositol-3-kinase
AKT: Protein kinase B
HFD: High-fat diet
LGBF: *Lophatherum gracile* Brongn. flavonoids
STZ: Streptozotocin
FBG: Fasting blood glucose
TC: Total cholesterol
TG: Triglyceride
LC-MS: Liquid chromatograph-mass spectrometer
PPI: protein-protein interaction
GO: Gene Ontology
KEGG: Kyoto Encyclopedia of Genes and Genomes
BP: Biological processes
CC: Cellular components
MF: Molecular functions
OGTT: Oral glucose tolerance test
AUC: Area under the curve
ITT: Insulin tolerance test
HOMA-IR: The homeostatic model assessment of insulin resistance
HDL-C: High-density lipoprotein cholesterol
AST: Alanine transaminase
ALT: Alanine transaminase.

## Data Availability

The data that support the findings of this study are available from the corresponding author upon reasonable request.

## Disclosure

Jian-Hua Zheng and Song-Xia Lin should be regarded as co-first authors

## Conflicts of Interest

All the authors declare that there are no conflicts of interest.

## Authors' Contributions

Jian-Hua Zheng was responsible for methodology and wrote the original draft. Song-Xia Lin was responsible for methodology and investigation and wrote the original draft. Xiao-Yi Li was responsible for formal analysis, methodology, and conceptualization. Chun-Yan Shen was responsible for investigation and conceptualization and reviewed and edited the draft. Shao-Wei Zheng was responsible for investigation and supervision and reviewed and edited the draft. Wen-Bin Chen was responsible for funding acquisition and project administration and reviewed and edited the draft. Jian-Hua Zheng and Song-Xia Lin contributed to the work equally.

## Acknowledgments

The authors gratefully acknowledge the financial support from the National Natural Science Foundation of China (82003908), Natural Science Foundation of Guangdong Province (2023A1515010720), Drug Administration of Guangdong Province (2022TDB37), Guangdong Basic and Applied Basic Research Foundation (2022A1515140046), and Huizhou Priority Clinical Speciality Cultivation Project (Orthopedics and Sports Medicine).

## References

[1] W. J. Sha, B. Zhao, H. Z. Wei et al., "Astragalus polysaccharide ameliorates vascular endothelial dysfunction by stimulating macrophage M2 polarization via potentiating Nrf2/HO-1 signaling pathway," *Phytomedicine*, vol. 112, Article ID 154667, 2023.

[2] D. Tawulie, L. L. Jin, X. Shang et al., "Jiang-Tang-San-Huang pill alleviates type 2 diabetes mellitus through modulating the gut microbiota and bile acids metabolism," *Phytomedicine*, vol. 113, Article ID 154733, 2023.

[3] S. Srinivasan and J. Todd, "The genetics of type 2 diabetes in youth: where we are and the road ahead," *The Journal of Pediatrics*, vol. 247, pp. 17–21, 2022.

[4] B. J. Hoogwerf, "Statins may increase diabetes, but benefit still outweighs risk," *Cleveland Clinic Journal of Medicine*, vol. 90, no. 1, pp. 53–62, 2023.

[5] S. H. Lee, S. Y. Park, and C. S. Choi, "Insulin resistance: from mechanisms to therapeutic strategies," *Diabetes & Metabolism J*, vol. 46, no. 1, pp. 15–37, 2022.

[6] Z. T. Zhang, W. J. He, S. M. Deng et al., "Trilobatin alleviates non-alcoholic fatty liver disease in high-fat diet plus streptozotocin-induced diabetic mice by suppressing NLRP3 inflammasome activation," *European Journal of Pharmacology*, vol. 933, Article ID 175291, 2022.

[7] Z. H. Dou, C. Liu, X. H. Feng et al., "Camel whey protein (CWP) ameliorates liver injury in type 2 diabetes mellitus rats and insulin resistance (IR) in HepG2 cells via activation of the PI3K/Akt signaling pathway," *Food and Function*, vol. 13, no. 1, pp. 255–269, 2022.

[8] Y. Shao, Q. N. Wu, J. A. Duan, W. Yue, W. Gu, and X. S. Wang, "Optimisation of the solvent extraction of bioactive compounds from Lophatherum gracile Brongn. using response surface methodology and HPLC-PAD coupled with pre-column antioxidant assay," *Analytical Methods*, vol. 6, no. 1, pp. 170–177, 2014.

[9] X. K. Liu, Y. Wang, W. Ge, G. Z. Cai, Y. L. Guo, and J. Y. Gong, "Spectrum-effect relationship between ultra-high-performance liquid chromatography fingerprints and antioxidant activities of Lophatherum gracile Brongn," *Food Science and Nutrition*, vol. 10, no. 5, pp. 1592–1601, 2022.

[10] K. H. Lai, P. J. Chen, C. C. Chen et al., "Lophatherum gracile Brongn. attenuates neutrophilic inflammation through inhibition of JNK and calcium," *Journal of Ethnopharmacology*, vol. 264, Article ID 113224, 2021.

[11] S. J. Lee, S. A. Jang, S. C. Kim, J. A. Ryuk, and H. Ha, "Lophatherum gracile bronghiart suppresses receptor activator of nuclear factor kappa-b ligand-stimulated osteoclastogenesis and prevents ovariectomy-induced osteoporosis," *International Journal of Molecular Sciences*, vol. 23, no. 22, Article ID 13942, 2022.

[12] C. Y. Shen, Y. F. Hao, Z. X. Hao et al., "Flavonoids from Rosa davurica Pall. fruits prevent high-fat diet-induced obesity and liver injury via modulation of the gut microbiota in mice," *Food and Function*, vol. 12, no. 20, pp. 10097–10106, 2021.

[13] H. X. Gao, H. Y. Liang, N. Chen, B. Shi, and W. C. Zeng, "Potential of phenolic compounds in Ligustrum robustum (Rxob.) Blume as antioxidant and lipase inhibitors: multi-spectroscopic methods and molecular docking," *Journal of Food Science*, vol. 87, no. 2, pp. 651–663, 2022.

[14] X. Y. Li, Z. Wang, J. G. Jiang, and C. Y. Shen, "Role of polyphenols from Polygonum multiflorum Caulis in obesity-related disorders," *Journal of Ethnopharmacology*, vol. 294, Article ID 115378, 2022.

[15] P. Zeng, Y. Yi, H. F. Su et al., "Key phytochemicals and biological functions of chuanxiong rhizoma against ischemic stroke: a network pharmacology and experimental assessment," *Frontiers in Pharmacology*, vol. 12, Article ID 758049, 2021.

[16] J. Q. Peng, K. Yang, H. Y. Tian et al., "The mechanisms of Qizhu Tangshen formula in the treatment of diabetic kidney disease: network pharmacology, machine learning, molecular docking and experimental assessment," *Phytomedicine*, vol. 108, Article ID 154525, 2023.

[17] E. R. Gilbert, Z. Fu, and D. Liu, "Development of a nongenetic mouse model of type 2 diabetes," *Experimental Diabetes Research*, vol. 2011, Article ID 416254, 12 pages, 2011.

[18] H. M. Abdou, F. A. Hamaad, E. Y. Ali, and M. H. Ghoneum, "Antidiabetic efficacy of trifolium alexandrinum extracts hesperetin and quercetin in ameliorating carbohydrate metabolism and activating IR and AMPK signaling in the pancreatic tissues of diabetic rats," *Biomedicine and Pharmacotherapy*, vol. 149, Article ID 112838, 2022.

[19] S. Lee, H. M. Ko, W. Jee, H. Kim, W. Chung, and H. Jang, "Isosinensetin stimulates glucagon-like peptide-1 secretion

via activation of hTAS2R50 and the G$\beta\gamma$-mediated signaling pathway," *International Journal of Molecular Sciences*, vol. 24, no. 4, p. 3682, 2023.

[20] D. Liu, X. Cao, Y. Kong, T. Mu, and J. Liu, "Inhibitory mechanism of sinensetin on $\alpha$-glucosidase and non-enzymatic glycation: insights from spectroscopy and molecular docking analyses," *International Journal of Biological Macromolecules*, vol. 166, pp. 259–267, 2021.

[21] P. Sun, R. Huang, Z. Qin, and F. Liu, "Influence of tangeretin on the exponential regression of inflammation and oxidative stress in streptozotocin-induced diabetic nephropathy," *Applied Biochemistry and Biotechnology*, vol. 194, no. 9, pp. 3914–3929, 2022.

[22] S. Yuan, Z. Ye, Y. Li et al., "Hypoglycemic effect of nobiletin via regulation of islet $\beta$-cell mitophagy and gut microbiota homeostasis in streptozocin-challenged mice," *Journal of Agricultural and Food Chemistry*, vol. 70, no. 19, pp. 5805–5818, 2022.

[23] T. D. Muller, M. Bluher, M. H. Tschop, and R. D. DiMarchi, "Anti-obesity drug discovery: advances and challenges," *Nature Reviews Drug Discovery*, vol. 21, no. 3, pp. 201–223, 2022.

[24] X. B. Yang, X. S. Li, Q. Y. Lin, and Q. F. Xu, "Up-regulation of microRNA-203 inhibits myocardial fibrosis and oxidative stress in mice with diabetic cardiomyopathy through the inhibition of PI3K/Akt signaling pathway via PIK3CA," *Gene*, vol. 715, Article ID 143995, 2019.

[25] X. J. Huang, G. H. Liu, J. Guo, and Z. Q. Su, "The PI3K/AKT pathway in obesity and type 2 diabetes," *International Journal of Biological Sciences*, vol. 14, no. 11, pp. 1483–1496, 2018.

[26] M. J. Watt, P. M. Miotto, W. De Nardo, and M. K. Montgomery, "The liver as an endocrine organ-linking NAFLD and insulin resistance," *Endocrine Reviews*, vol. 40, no. 5, pp. 1367–1393, 2019.

[27] Y. Yang, X. Jia, M. Qu et al., "Exploring the potential of treating chronic liver disease targeting the PI3K/Akt pathway and polarization mechanism of macrophages," *Heliyon*, vol. 9, no. 6, 2023.

[28] N. Chen, R. Cao, Z. Zhang, S. Zhou, and S. Hu, "Sleeve gastrectomy improves hepatic glucose metabolism by downregulating FBXO2 and activating the PI3K-AKT pathway," *International Journal of Molecular Sciences*, vol. 24, no. 6, p. 5544, 2023.

[29] J. Zhou, Y. Shi, C. Yang et al., "$\gamma$-glutamylcysteine alleviates insulin resistance and hepatic steatosis by regulating adenylate cyclase and IGF-1R/IRS1/PI3K/Akt signaling pathways," *The Journal of Nutritional Biochemistry*, vol. 119, Article ID 109404, 2023.

[30] S. Niranjan, B. E. E. Phillips, and N. Giannoukakis, "Uncoupling hepatic insulin resistance-hepatic inflammation to improve insulin sensitivity and to prevent impaired metabolism-associated fatty liver disease in type 2 diabetes," *Frontiers in Endocrinology*, vol. 14, Article ID 1193373, 2023.

[31] M. P. Czech, "Insulin action and resistance in obesity and type 2 diabetes," *Nature Medicine*, vol. 23, no. 7, pp. 804–814, 2017.

[32] M. Acosta-Martinez and M. Z. Cabail, "The PI3K/Akt pathway in meta-inflammation," *International Journal of Molecular Sciences*, vol. 23, Article ID 15330, 2022.

[33] T. Rohm, D. T. Meier, J. M. Olefsky, and M. Y. Donath, "Inflammation in obesity, diabetes, and related disorders," *Immunity*, vol. 55, no. 1, pp. 31–55, 2022.

[34] O. Osborn and J. M. Olefsky, "The cellular and signaling networks linking the immune system and metabolism in disease," *Nature Medicine*, vol. 18, no. 3, pp. 363–374, 2012.